

Inclusive measurement of quasifree (p,xn) charge exchange reactions on bismuth from 62 to 800 MeV

J. M. D'Auria, M. Dombisky, and G. Sheffer*

Department of Chemistry, Simon Fraser University, Burnaby, British Columbia, Canada V5A 1S6

T. E. Ward[†] and H. J. Karwowski[‡]

Indiana University Cyclotron Facility, Indiana University, Bloomington, Indiana 47401

A. I. Yavin

Department of Physics and Astronomy, Tel Aviv University, Tel Aviv, Israel

J. L. Clark[§]

Los Alamos National Laboratory, Los Alamos, New Mexico 87545

(Received 21 February 1984)

The total inclusive (p,xn) charge exchange reaction cross section on bismuth from 62 to 800 MeV was measured using activation and radiochemical techniques. These data for products with as many as 14 neutrons removed from the coherent product display the simple E^{-1} dependence of the total cross section with incident projectile energy. The distribution of charge exchange products is discussed in terms of quasifree processes in (p,n) reactions. A model comparison between the data and an intranuclear cascade calculation was satisfactory as evidenced by reproducing the energy dependence, cross section magnitude, and mass yields for products up to 14 neutrons removed. Better agreement between the model and data were obtained with mean-free paths of nucleons in nuclear matter twice as long as the one derived from nucleon-nucleon scattering.

I. INTRODUCTION

The extent to which and manner in which the energy, angular, and momentum transfer dependence of a reaction cross section reflects various aspects of the kinematics, nuclear structure, or reaction mechanism depends specifically on the initial interaction. The majority of spallation reactions are reasonably described by an initial cascade of several fast nucleons followed by evaporation of a large number of particles. Such processes obscure the initial interaction due to averaging and statistical effects; in particular, the angular and momentum dependence of simple inclusive experiments is lost. However, the energy dependence of specific nuclear reactions has proven to be of considerable value in understanding intermediate energy, proton-induced reactions.¹ Excitation functions for the production of specific nuclei (angle integrated and averaged over all bound states) through a definite reaction path are still of considerable interest and value.²

Intermediate energy (≥ 50 MeV/nucleon), proton-induced reactions leading to residual nuclei a few nucleons removed from the target are believed to proceed by the rather simple two-step mechanism described above, namely an initial direct nucleon-nucleon interaction (with possible cascade nucleon emission) followed by a statistical type of nucleonic emission leading to the specific product.^{1,3} The (p,xn) reactions are of some interest primarily because of the energy and momentum restrictions of the initial (p,n) charge exchange. The observed energy dependence of (p,n) reactions below 1 GeV on a variety of target nuclei has been observed to vary approximately inverse in

bombarding energy³⁻⁶ and similar to that of the free-particle p-n scattering cross section.^{5,7} These simple dependences were also observed for (p,xn)-type reactions with x as large as 6 (Refs. 7 and 8), which supports the suggestion of initial quasifree p-n charge exchange scattering, resulting in an excited nucleus which subsequently may statistically emit one or more neutrons.^{2-5,7-9} Little data exists for (p,xn) reactions for energies above 100 MeV or indeed for large values of x . Clearly, the more neutrons emitted, the higher the excitation energies necessary in the initial, projectile energy dependent step. In the present study the excitation functions for the production of polonium products as light as 196 from the ²⁰⁹Bi target, i.e., (p,xn) reactions on bismuth with x as large as 14, were measured at incident proton energies up to 800 MeV. These data were compared with calculations of an intranuclear cascade program examining the energy and mass yields for this reaction from 60 to 800 MeV.

II. EXPERIMENTAL

The total reaction cross sections for the long-lived ($t_{1/2} \geq 20$ min) polonium nuclides produced in the ²⁰⁹Bi(p,xn) reaction were obtained by measurements of residual alpha activities of radiochemically separated polonium samples. Irradiations of thin (≤ 10 mg/cm²) bismuth foils were performed at the Indiana University Cyclotron Facility (IUCF) for incident proton energies from 62 to 200 MeV, at the TRIUMF Cyclotron Facility (Vancouver, Canada) for those from 185 to 500 MeV, and

at Los Alamos Meson Physics Facility (LAMPF) for a proton energy at 800 MeV. Irradiation times were typically of the order of one hour while integration of the beam current was made using a Faraday cup or the simultaneous production of ^{24}Na in a thin ($\approx 2 \text{ mg/cm}^2$) aluminum catcher of the same dimensions as the bismuth target.¹¹ Recoiling ^{24}Na nuclides were taken into account¹² along with disruptions during irradiation. Chemical separations for polonium were performed approximately 1 h after irradiation. Further details of the techniques used for the longer-lived Po isotopes, including details of the radiochemical polonium separation, the alpha detection system, etc., are given elsewhere.¹⁰ Information on the alpha decay of the polonium isotopes measured in the study are presented in Table I.

A different, more direct approach was utilized to measure the yield of short-lived polonium isotopes. These were only performed at TRIUMF. A very thin ($\approx 100 \text{ } \mu\text{g/cm}^2$) deposit of bismuth was evaporated onto a thin ($\approx 200 \text{ } \mu\text{g/cm}^2$) carbon backing. This target was mounted on a movable arm in a vacuum chamber with the bismuth side downstream of the incident beam (0°). This target arm could be remotely moved and positioned in front of a Si surface barrier detector (30°). A timed cycle could be repeated although the proton beam remained on continuously. It took approximately 1 sec/deg for the arm to move. Multispectral alpha counting could then be performed in the standard manner. Figure 1 displays the (direct) alpha spectrum observed for a $2 \text{ } \mu\text{A}$ beam proton

TABLE I. Alpha decay parameters of polonium isotopes. (Reference 13, except where indicated.)

<i>A</i>	$T_{1/2}$	I^π	E_α (MeV) ^a	<i>I</i> (%)
196	5.5 sec	0^+	6.52	100
197	58 sec		6.280	90
197 <i>m</i>	26 sec		6.385	100
198	1.78 min	0^+	6.183 ^b	70
199	5.2 min	$(\frac{3}{2}^-)$	5.952	12
199 <i>m</i>	4.2 min	$(\frac{13}{2}^+)$	6.060	39
200	11.6 min	0^+	5.864	14
201	15.2 min	$(\frac{3}{2}^-)$	5.68	1.6
201 <i>m</i>	8.9 min	$(\frac{13}{2}^+)$	5.786 ^b	2.9
202	44 min	0^+	5.588	2.0
203	33 min	$\frac{5}{2}^-$	5.38	0.1
203 <i>m</i>	1.2 min	$(\frac{13}{2}^+)$		≈ 0
204	3.57 h	0^+	5.377	0.62
205	1.80 h	$\frac{5}{2}^-$	5.240	0.49
206	8.83 d	0^+	5.224	5.45
207	5.7 h	$\frac{5}{2}^-$	5.12	0.008
208	2.897 yr	0^+	5.114	100
209	102 yr	$\frac{1}{2}^-$	4.884	99.74

^aMean values.

^bThe observed energy here for ^{198}Po was 6.177 and for $^{201}\text{Po}^m$ was 5.778 MeV in agreement with Ref. 15.

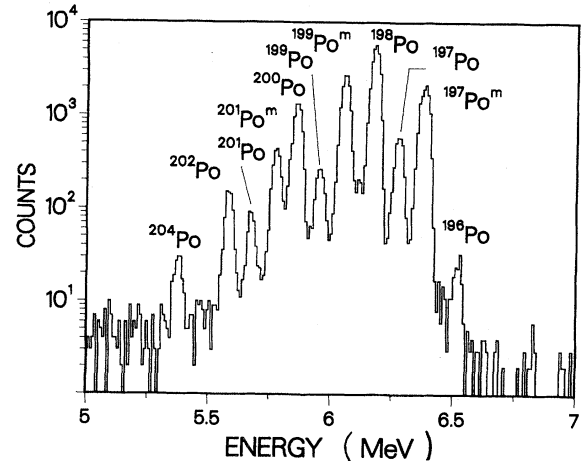


FIG. 1. The summed (for six cycles) alpha spectrum obtained for a 1 min counting interval directly following the irradiation of a thin bismuth foil with 210 MeV protons for 1 min and a wait time of 0.5 min. Identification of these peaks was based upon observed energies and half-lives, and comparison with literature values (Ref. 13).

energy of 210 MeV. The cycling sequence was an irradiation time of 1.0 min, a moving time of 0.5 min, and a counting time of 1 min/spectra. This spectrum represents the first in a series of six spectra collected for six cycles. As these data were only used to determine production cross section ratios, beam current was not monitored simultaneously. All alpha spectra were analyzed using the SAMPO code¹⁴ on an IBM 370-55 system. Final isotopic identification was based upon the unique combination of alpha energy and nuclide decay half-life.

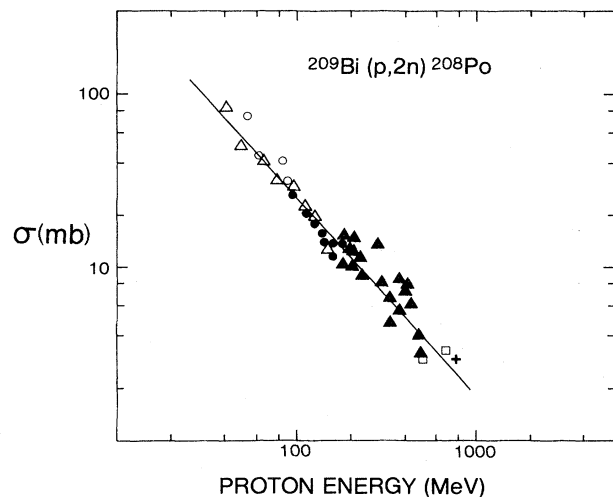


FIG. 2. Displayed here (as taken from Ref. 10) are all of the known values for the total reaction cross sections for the production of ^{208}Po from a bismuth target as a function of incident proton energy (log-log). See Ref. 10 for information on the sources for these data. An additional data point (+) measured here is indicated at 800 MeV. Error bars are not displayed for clarity but the data from the present study [IUCF (Δ), TRIUMF (\bullet), and LAMPF (+)] have a total error of about 20%. The solid line represents a fit to the data using the relationship $\sigma = a \cdot E^{-b}$ (see Table V and the text).

III. RESULTS

Absolute cross sections for the production of ^{208}Po and ^{206}Po from 62 to 480 MeV were reported in an earlier publication (Table II of Ref. 10). Displayed here in Fig. 2 are these data (for ^{208}Po) along with all other reported measurements of σ_T for the production of ^{208}Po from ^{209}Bi with protons of energies between 62 and 800 MeV. Included is one additional measurement (at 800 MeV) performed by this group since the earlier publication.¹⁰ The error in the data measured here is approximately 23% on each point, arising from the errors in the determination of chemical efficiency (20%), beam integration (7%), detection solid angle (5%), statistics (5%), and target thickness (5%). As is discussed in the earlier study,¹⁰ there is apparently a smooth and not unexpected energy dependence (solid line in Fig. 1) between σ_T and E_p ; namely, $\sigma_T = a/E^b$ or

$$\log \sigma_T = \log a - b \log E, \quad (1)$$

with $\log a = 3.66 \pm 0.15$ and $b = 1.134 \pm 0.06$. Presented in Table II then are the measured cross section ratios (mean values) for ^{209}Po , ^{206}Po , ^{204}Po , and ^{202}Po as compared to ^{208}Po . The relative error ($\approx 5\%$) is primarily due to statistics. The individual errors, due to errors in the reported alpha branching rates, were not included (except

TABLE II. Ratios (mean values) of cross sections for production of polonium isotopes (202–209). [The cross section for the production of a polonium isotope of mass number, A , can be calculated by the equation, $\text{ratio} \times \sigma_{\text{calc}}(^{208}\text{Po})$, where $\sigma_{\text{calc}} = a \cdot E^b$ and a and b are given in Table IV and Ref. 10.]

E_p (MeV)	$\frac{209}{208}$	$\frac{206}{208}$	$\frac{204}{208}$	$\frac{202}{208}$
62		3.17	4.7	
80	0.18	2.06	5.3	7.6
95	0.21	2.25	4.4	4.3
115	0.20	2.16	3.7	
125	0.20	1.97	3.3	3.1
136	0.22	2.25	3.4	4.3
144	0.27	2.18	3.1	3.3
150	0.21	1.72	2.5	2.1
154	0.24	1.68	3.4	1.1
160	0.33	1.95		
170		1.79	2.0	
179		1.98	2.8	2.0
183	0.30	1.97	2.5	1.8
190	0.29	2.03	2.5	2.0
200	0.31	1.81	2.7	2.2
210	0.27	1.91	2.4	1.6
225	0.28	1.95	2.3	1.5
237	0.27	2.15	2.7	2.0
280	0.28	1.79	2.3	1.5
300	0.33	2.04	2.4	1.3
330	0.29	1.95	2.5	1.6
367	0.36	1.94		
400	0.29	1.94	2.3	1.4
430	0.33	1.95		
480	0.36	1.94	2.4	2.2
800	0.23	1.85	2.4	1.4

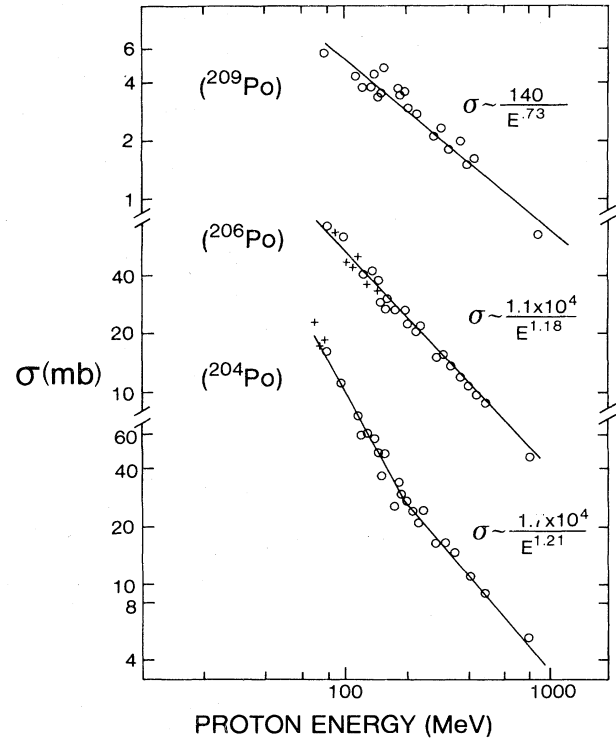


FIG. 3. The total cross sections (open circles) for the production of ^{209}Po (upper), and ^{206}Po and ^{204}Po (lower) as a function of incident proton energy (log-log). These values were deduced from the product of the cross section ratios (see Table II) and $\sigma_{\text{calc}}(^{208}\text{Po}) (= a \cdot E^{-b})$ (see Table IV and Ref. 10). Data [corrected for different alpha branching (see ratios)] taken from literature values (Ref. 17) are also presented (crosses) for comparison. The indicated solid lines are fits to these data, using the relationship $\sigma = a \cdot E^{-b}$ (see Table IV).

for ^{202}Po). The cross section then for any of these can be obtained by multiplication with the calculated cross section for ^{208}Po [Eq. (1)]. Displayed in Fig. 3 are some of these excitation functions. Also included in Fig. 3, where appropriate, are measurements from other published reports for comparison.

Table III presents the cross section ratios for the shorter-lived polonium isotopes measured directly (without chemistry). These are compared to ^{202}Po , rather than ^{208}Po , since the latter was not observed in significant amounts simultaneously due to the short cycling times. The errors in these cases included errors in reported alpha branching ratios and half-lives in addition to statistics. These data along with those in Table II are presented graphically in Fig. 4 for certain incident beam energies and in effect as a function of the number of neutrons removed from a coherent (^{210}Po) product. A standard Gaussian expression with a normalization amplitude (N), a full-width at half-maximum (FWHM) in units of A , and a most probable mass (A_p) was used to fit these mass yield distributions. These fitted parameters are presented in Table IV.

Finally, an expression of the same form as Eq. (1) was used to fit all of the excitation functions (e.g., Fig. 3) and

TABLE III. Cross section ratios ($\times 10$) for production of polonium isotopes (196–201). [These ratios should be *divided* by a factor of 10 to yield the correct value; the errors presented include statistical errors and quoted errors in published alpha branching ratios and half-lives (Ref. 13). See footnote for Table II; $\sigma_{\text{calc}}(^{202}\text{Po}) = a \cdot E^b$, where empirically determined values for a and b are given in Table IV.]

E_p (MeV)	$\frac{201 m}{202}$	$\frac{200}{202}$	$\frac{199 m}{202}$	$\frac{199}{202}$	$\frac{198}{202}$	$\frac{197 m}{202}$	$\frac{197}{202}$	$\frac{196}{202}$
210	8.1 ± 0.6	6.3 ± 1.4	3.0 ± 0.3	0.84 ± 0.14	2.5 ± 0.3	0.75 ± 0.3	0.19 ± 0.02	0.6 ± 0.1
300	4.7 ± 0.6	3.8 ± 0.6	1.5 ± 0.1	0.29 ± 0.06	0.9 ± 0.1	0.56 ± 0.1	0.09 ± 0.02	
400	7.1 ± 0.8	5.3 ± 0.6	2.1 ± 0.2	0.56 ± 0.09	2.0 ± 0.2	0.33 ± 0.08	0.15 ± 0.03	
450	9.6 ± 0.9	7.7 ± 0.6	3.3 ± 0.3	1.1 ± 0.12	2.7 ± 0.3	0.39 ± 0.05	0.11 ± 0.02	0.5 ± 0.5
480	7.6 ± 0.6	5.4 ± 0.4	2.4 ± 0.2	0.65 ± 0.06	1.9 ± 0.2	0.69 ± 0.07	0.12 ± 0.02	0.7 ± 0.2

Table V presents the values of a and b as determined from a least squares analysis. The correlation coefficient (R^2) is also given. It should be noted that in some cases, e.g., ^{204}Po , only the higher energy (noncompound nucleus⁹) data were used (see Table V).

IV. DISCUSSION

These data exhibit certain interesting features which allow the development of a consistent but not surprising picture regarding the overall mechanism of such processes, despite the lack of the specific kinematical information. These features include the following:

(1) the remarkably simple and similar dependence observed between the total cross section for the production of any polonium isotopes, and the incident proton energy

(see Table IV);

(2) the distinct difference in the value of the exponential factor (b) for the production of ^{209}Po , i.e., 0.73, and that for ^{208}Po , 1.13, as compared to the smooth variation from ^{208}Po to ^{202}Po (see Table V);

(3) the almost independent behavior of the most probable polonium product mass (A_p) with respect to incident proton energy, along with the simple Gaussian shape (see Fig. 4 and Table IV) of the mass yield data.

These data are similar although more complete as compared to those of Caretto and co-workers in a series of studies^{3,5,8,9} and to those of LeBeyec and Lefort.^{1,16} The suggested mechanism involves an initial, fast, quasifree p-n charge exchange scattering, followed by a statistical emission of $(x-1)$ neutrons depending upon the excitation energy deposited. The contribution from the fast step involving emission of a second neutron is considered small.⁸ This picture is consistent with the results of the present study as will be discussed below. A comparison with calculations from an intranuclear cascade approach will also be presented.

It is somewhat surprising to observe the simple $1/E$ dependence up to such a high projectile energy and for products so far removed from the coherent product. As noted by Treytl and Caretto, Jr.⁵ the observed exponential dependence for the exclusive total (p,n) reaction cross section decreases from 1.3 to about 0.75 as the target mass increases. In the case of $^7\text{Li}(p,n)^7\text{Be}$ a value of about 1.1 is observed and the simple dependence is attributed to (a) the trivial kinematic factor $1/k_p k_n$, and (b) the effective cancellation of two very energy dependent terms in the reaction matrix elements, following a DWIA analysis based upon the free nucleon-nucleon t matrix.⁶ As noted by Karol¹⁷ based upon the semiclassical approach of Sternheim-Silbar, and production cross section up to 150 MeV for the residual nuclei of a (p,n) reaction can be written as

$$\sigma(p,n) \approx \frac{1}{T_p^{0.8}}$$

in the case of the ^{11}C target. A similar situation clearly exists in the present study (see Table IV). It should be noted that the total n-p free nucleon cross section goes as $T_p^{-1.1}$ up to a projectile energy of about 160 MeV and then levels off. On the other hand, the n-p backward elastic cross section,^{18,19} otherwise referred to as the p-n

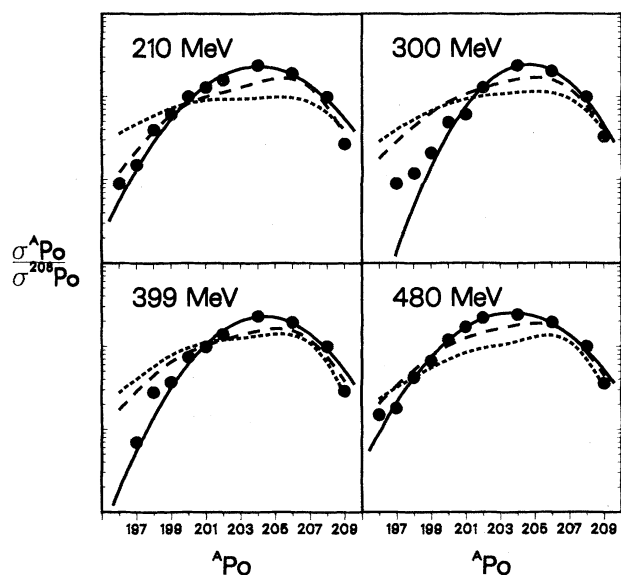


FIG. 4. Displayed here (solid points) are the measured cross-section ratios to that of ^{208}Po as a function of A_{Po} , the polonium isotopic product at different incident proton energies. The solid lines here represent Gaussian fits to these distributions, with the mean deduced to be 204.1 ± 0.05 (see Table V). Calculations using the intranuclear cascade model for two values of the mean free path (λ), $\lambda=1$ and $\lambda=2$ (see the text for explanation) are given by the dotted and dashed lines, respectively.

TABLE IV. Characteristics of mass yield data assuming a Gaussian fit (see the text).

Proton energy (MeV)	Most probable mass (A_p)	FWHM (A units)	Normalization amplitude (N)
210	204.0±0.15	6.9±1.4	2.31±0.12
300	204.7±0.1	5.6±1.0	2.45±0.01
399	204.4±0.1	6.3±1.3	2.28±0.11
450	203.9±0.2	7.2±1.6	2.29±0.13
480	203.7±0.1	7.0±0.8	2.52±0.07
Mean	204.1±0.05	6.6±0.5	

charge exchange scattering cross section, does display a $T_p^{-1.2}$ dependence up to a projectile energy of at least 700 MeV. Thus, the quasifree p-n scattering appears to be the determining step leading to the production of these (p,xn) products, with the exponential change to 0.73 for the (p,n) reaction on bismuth attributable to nuclear medium effects. Intranuclear cascade calculations discussed later do exhibit better agreement with data presented here with an increase in the mean free path used.

The gradual change from 1.1 to 1.3 in the exponential dependence for the production of ^{208}Po to ^{202}Po (Table V) probably reflects the increase in the maximum allowable scattering angle in the initial p-n charge exchange process. This, in turn, would result in higher momentum transfers, higher excitation energies, and, in turn, emission of more neutrons. In this study products at least 14 neutrons removed from the coherent product, or requiring at least on the order of 120 MeV excitation energies, were observed with similar projectile energy dependences. The rather abrupt change for the (p,2n) product as compared to the (p,n) product probably reflects the different mechanism of their production. If two fast cascade nucleons were emitted primarily, then the slopes of the (p,n) and (p,2n) products would be expected to be similar. The steeper dependence on the incident energy for the second step, the statistical emission step, probably reflects competition from other emission processes.

The most probable product observed in this study for incident energies greater than 200 MeV is ^{204}Po (see Table IV). This reflects the emission of five neutrons following an initial fast (p,n) charge exchange process. The separation energy of this product is about 55 MeV, yielding a most probable momentum transfer

$$\langle \langle E_{\text{sep}} \rangle \rangle = \langle P_{m\text{p}} \rangle^2 / 2m_N \text{ of } \langle P_{m\text{p}} \rangle = 320 \text{ MeV}/c .$$

TABLE V. Statistical parameters for fit of equation $\sigma(A) = a \cdot E^b$ (σ in mb and E in MeV).

A	a	b	R^2
209	139.35	-0.729	0.87
208	4570.9±4 %	-1.134±0.06	0.97
206 ^a	11 381	-1.178	0.98
204 ^b	17 236.7	-1.209	0.93
202 ^c	19 858.4	-1.300	0.84

^aOnly used data for $E_p \geq 80$ MeV.

^bOnly used data for $E_p \geq 150$ MeV.

^cOnly used data for $E_p \geq 180$ MeV.

This value is consistent with other proton-nucleus studies at intermediate energies which have been examining the linear momentum transfer in the intranuclear cascade process.²⁰⁻²² The observed mass yield data along with the most probable product are essentially independent of incident proton energy (see Fig. 4 and Table IV). This reflects the fact that the product of the transferred momentum distribution (excitation energy) of the initial step and the subsequent probability for emission for all of these products is essentially a constant. Since the latter are very (excitation) energy dependent functions, the distribution of the transferred momentum in the initial p-n charge exchange step is probably quite broad. The similarity between these results and the mass-yield data for polonium isotopes resulting from a proton transfer process in the interaction of energetic ^{12}C projectiles (86 MeV/nucleon) with bismuth²³ is consistent with broad momentum distribution from an initial fast interaction, followed by a statistical emission process.

In Fig. 4 are also displayed the results of an intranuclear cascade VEGAS code²⁴ calculation for two values of the mean free path (MFP). The calculations were performed by incorporating a nonconstant nuclear density distribution which was run in the option in which reflection and refraction are ignored at the density step boundary. Subsequent evaporation computations were performed using the Dostrovsky, Fraenkel, and Friedlander (DFF) code,²⁵ which utilizes the Monte Carlo technique to calculate evaporation of particles using the Weisskopf evaporation formula. The input parameters used for calculations in the VEGAS and DFF codes were chosen to be the same as those which appear to give a good account of the inclusive production cross section for the p + Ni reaction in the 80–164 MeV energy range.^{26,27} The only parameter varied in the present calculations is the value of the mean free path, λ , of the fast nucleon in the nucleus, which in the VEGAS code is derived from the free nucleon-nucleon scattering. As indicated in Fig. 4, two values were used for the MFP: the standard λ (see Ref. 24) and λ multiplied by a factor of 2.

The estimates of the MFP vary considerably depending on the method used in its determination. Gadioli *et al.*²⁸ assume $\lambda = 17$ fm to explain the proton spectrum observed in the $^{89}\text{Y}(p,p')$ reaction. McKeown *et al.*²⁹ assumed $\lambda = 4-9$ fm for 100 MeV nucleons, whereas Chang and Hüfner³⁰ use $\lambda = 3-5$ fm for a 10–100 MeV nucleon energy range. We did not attempt to fit the value of λ to our data, although it is evident from Fig. 4 that increasing

λ does improve the agreement with the experiment for all residual masses at all proton bombarding energies. Similar improvement in predictions of the residue production cross sections for the p + Ni reaction was obtained²⁶ when the MFP used in exciton model calculations was doubled.

It was anticipated that multichance fission-evaporation competition might alter the calculated cross section distribution, especially for the very mass deficient residues (see Fig. 4). Calculations of the fission-evaporation competition were performed using the MBEGAT code³¹ with the parameter set described in detail in Ref. 32. As expected, the fission process will only be non-negligible at high angular momentum and high excitation energies. Exact distributions of excitation energy (E) vs angular momentum (J) of residues after the fast phase of the reaction are not known. Therefore, we have calculated fission cross sections for several selected values of E and J from which we can estimate the effect of fission on the final residue production cross section.

The ratio of fission widths to total widths $\Gamma_f/\Gamma_{\text{tot}}$ as calculated by the MBEGAT code varies for ²¹⁰Po from 0.031 for $E^*=90$ MeV and $J=30\hbar$ to 0.008 for $E^*=50$ MeV and $J=10\hbar$. The fission probability increases with Z^2/A of the residue, i.e., with decreasing neutron number. For example, for ²⁰⁵Po $\Gamma_f/\Gamma_{\text{tot}}$ varies from 0.057 for

$E^*=90$ MeV, $J=30\hbar$ to 0.026 for $E^*=50$ MeV, $J=10\hbar$. There is also a competing effect of decreasing average excitation energy (~ 10 MeV per emitted neutron) and decreasing angular momentum which tends to keep an average $\Gamma_f/\Gamma_{\text{tot}}$ at a constant value of 0.03 for $A \leq 203$ nuclei. We can therefore estimate that fission competition will, on the average, decrease the residue production cross section for Po isotopes by $\sim 7\%$ for ²⁰⁸Po, to $\sim 20\%$ for ²⁰³Po, and $\sim 35\%$ for ¹⁹⁷Po. These corrections have not been applied to the calculated values shown in Fig. 4, but the correction is in the right direction for better agreement for the most deficient residues.

In summary, we have measured the total inclusive quasifree (p,xn) charge exchange reaction cross section on bismuth from 62–800 MeV. The results show the characteristic $1/E$ energy dependence of this reaction for x as large as 14. The results are in good agreement with an intranuclear cascade calculation reproducing the energy, mass yield curves, and absolute magnitude of the cross sections provided the MFP is a factor of 2 larger than the free nucleon-nucleon scattering value used in the calculation. The data are consistent with only one fast cascade nucleon emitted prior to evaporation processes and the most probable momentum transfer determined from the residue curves is $\langle P_{mp} \rangle = 320$ MeV/ c .

*Permanent address: TRIUMF, 4004 Wesbrook Mall, Vancouver, British Columbia, Canada V6T 2A3.

†Permanent address: Department of Chemistry, Indiana University, Bloomington, IN 47401.

‡Permanent address: Department of Physics, North Carolina State University, Triangle Park, NC 27607.

§Permanent address: General Physics Corporation, 1000 Century Plaza, Columbia, MD 21044.

¹For a review, see J. Hudis, in *Nuclear Chemistry*, edited by L. Yafee (Academic, New York, 1968), Vol. I, p. 169; M. LeFort, *Nuclear Chemistry* (Van Nostrand, London, 1968), Chap. 5.

²S. B. Kaufman and E. P. Steinberg, *Phys. Rev. C* **22**, 167 (1980).

³J. R. Grover and A. A. Caretto, Jr., *Annu. Rev. Nucl. Sci.* **14**, 51 (1964).

⁴R. C. Koch, Ph.D. thesis, University of Chicago, 1955.

⁵W. J. Treytl and A. A. Caretto, Jr., *Phys. Rev.* **146**, 836 (1966).

⁶T. E. Ward, C. C. Foster, G. E. Walker, J. Rapaport, and C. A. Goulding, *Phys. Rev. C* **25**, 762 (1982).

⁷J. B. Read and J. M. Miller, *Phys. Rev.* **140**, 623 (1965).

⁸L. B. Church and A. A. Caretto, Jr., *Phys. Rev.* **178**, 1732 (1969).

⁹W. J. Nickarz and A. A. Caretto, Jr., *Phys. Rev.* **178**, 1887 (1969).

¹⁰T. E. Ward, P. P. Singh, D. Friesel, A. Yavin, A. Doron, J. M. D'Auria, G. Sheffer, and M. Dillig, *Phys. Rev. C* **24**, 588 (1981).

¹¹J. B. Cumming, *Annu. Rev. Nucl. Sci.* **13**, 261 (1963).

¹²A. Poskanzer, J. B. Cumming, and R. Wolfgang, *Phys. Rev.* **129**, 374 (1963).

¹³*Table of Isotopes*, 7th ed., edited by C. M. Lederer and V. Shirley (Wiley, New York, 1978).

¹⁴J. T. Routti and S. G. Prussin, *Nucl. Instrum. Methods* **72**,

125 (1969).

¹⁵W. Treytl and K. Valli, *Nucl. Phys.* **A97**, 405 (1967).

¹⁶Y. LeBeyec and M. Lefort, *Nucl. Phys.* **A99**, 131 (1967).

¹⁷P. Karol, *Phys. Rev. C* **23**, 415 (1981).

¹⁸O. Benary and L. R. Price, Particle Data Group, University of California Radiation Laboratory Report UCRL-20000-NN, 1970.

¹⁹W. Hurster, T. Fisher, G. Hammel, K. Kern, M. Kleinschmidt, L. Lehman, H. Schmitt, L. Schmitt, and D. Shepard, *Phys. Lett.* **90B**, 367 (1980).

²⁰G. Mathews, B. G. Glagala, R. A. Moyle, and V. E. Viola, Jr., *Phys. Rev. C* **25**, 2181 (1982).

²¹F. Saint Laurent *et al.*, *Phys. Lett.* **110B**, 372 (1982).

²²L. Woo, K. Kwiatkowski, and V. E. Viola, Jr., *Phys. Lett.* **132B**, 283 (1983).

²³D. Molzahn, T. Lund, R. Brandt, E. Hagebo, I. R. Haldorsen, and C. R. Serre, *J. Radioanal. Chem.* **80**, 109 (1983).

²⁴J. M. Miller and G. Friedlander, *Phys. Rev.* **110**, 185 (1958); K. Chen, Z. Fraenkel, G. Friedlander, J. R. Grover, J. M. Miller, and Y. Shimamoto, *ibid.* **166**, 949 (1968).

²⁵L. Dostrovsky, Z. Fraenkel, and G. Friedlander, *Phys. Rev.* **116**, 683 (1959).

²⁶M. E. Sadler, P. P. Singh, J. Jastrzebski, L. L. Rutledge, and R. E. Segel, *Phys. Rev. C* **21**, 2303 (1980).

²⁷J. Jastrzebski, H. J. Karwowski, M. E. Sadler, and P. P. Singh, *Phys. Rev. C* **22**, 1443 (1980).

²⁸E. Gadioli *et al.*, *Phys. Lett.* **65B**, 311 (1976).

²⁹R. D. McKeown *et al.*, *Phys. Rev. Lett.* **44**, 1033 (1980).

³⁰H. C. Chang and J. Hüfner, *Nucl. Phys.* **A349**, 466 (1980).

³¹S. E. Vigdor, H. J. Karwowski, W. W. Jacobs, S. Kailas, P. P. Singh, F. Soga, and T. G. Throwe, *Phys. Rev. C* **26**, 1035 (1982).

³²S. E. Vigdor and H. J. Karwowski, *Phys. Rev. C* **26**, 1068 (1982).